ResearchGate

See discussions, stats, and author profiles for this publication at: https://www.researchgate.net/publication/228569403

Relevant parameters and finite amplitude effects in estuarine hydrodynamics

Article *in* Journal of Geophysical Research Atmospheres · October 2006

DOI: 10.1029/2005JC003104

CITATIONS
49

READS
329

3 authors:

Marco Toffolon
Università degli Studi di Trento
112 PUBLICATIONS **2,187** CITATIONS
SEE PROFILE

Gianluca Vignoli
23 PUBLICATIONS **263** CITATIONS
SEE PROFILE

Marco Tubino
Università degli Studi di Trento
108 PUBLICATIONS **3,349** CITATIONS
SEE PROFILE

Some of the authors of this publication are also working on these related projects:

Project Sustainability of small municipalities through local energy production View project

Project Science for Management of Ypacaraí Lake's Eutrophication (SMYLE) View project

All content following this page was uploaded by Gianluca Vignoli on 16 May 2014.

The user has requested enhancement of the downloaded file.

.

An edited version of this paper was published by AGU. Copyright (2006) American Geophysical Union.
Toffolon, M., G. Vignoli, and M. Tubino (2006), Relevant parameters and finite amplitude effects in estuarine hydrodynamics, *J. Geophys. Res.*, *111*, C10014, doi:10.1029/2005JC003104.
To view the published open abstract, go to http://www.agu.org/pubs/crossref/2006/2005JC003104.shtml

Relevant parameters and finite amplitude effects in estuarine hydrodynamics

Marco Toffolon, Gianluca Vignoli[1], and Marco Tubino
Department of Civil and Environmental Engineering, University of Trento, Italy

Abstract. The propagation of the tidal wave in convergent estuaries is investigated through a one-dimensional numerical model, which allows to consider the role of finite amplitude effects. The relevant dimensionless parameters characterizing estuarine hydrodynamics are given in terms of independent quantities, namely the geometry of the channel and the tidal forcing. Hence a suitable scale of velocity is derived, which covers both the cases of convergent and dissipative estuaries. Furthermore, the marginal conditions for tidal wave amplification, resulting from a balance between the damping effect of friction and the amplification due to channel convergence, are investigated. We show that the marginal curves can be given the form of power laws whose coefficients depend on the dimensionless tidal amplitude; the linear behavior predicted by analytical solutions is only recovered for vanishing values of the ratio between the tidal amplitude and the tidally averaged water depth. Finally, the proposed scale of velocity and that derived from the model of *Savenije and Veling* [2005] are tested against numerical results for a wide range of parameters.

1. Introduction

In this paper we tackle the problem of defining the relevant dimensionless parameters which govern estuarine hydrodynamics in terms of externally defined quantities, namely the large-scale geometrical properties of the estuary and the characteristics of the tidal forcing. We consider a widespread class of tidal environments, namely the well-mixed estuarine channels, where the tidal forcing is so strong that stratification does not occur. In this case the absence of the salt wedge allows one to consider a constant density of water and to describe the flow field using the usual equations of single-phase fluid. The hydrodynamics of such systems is strongly affected by the geometrical characteristics of the channel, in particular by the convergence of the cross-section, which is due to a landward decrease of the width and the average depth, and by the presence of intertidal areas. Understanding the relative role of the various mechanisms may help in interpreting the morphological response of such systems, for which several empirical relationships have been derived, like the *Jarret*'s [1976] law between tidal prism and channel cross-section. Furthermore, it allows one to evaluate the consequence of both natural and anthropogenic modifications.

[1]Now at CISMA, Bolzano, Italy.

Copyright by the American Geophysical Union.
0148-0227/09/$9.00

The problem has already received considerable attention (see for instance *Ippen* [1966], *Dronkers* [1964], *Parker* [1991], *Jay* [1991], *Friedrichs and Aubrey* [1994], *Friedrichs et al.* [1998], *Lanzoni and Seminara* [1998], *Savenije and Veling* [2005]) and various classifications of estuaries have been proposed in terms of their hydrodynamic characteristics, depending upon the relative role of friction, inertia and convergence of the cross-section.

In our work we analyze the hydrodynamical behavior of tidal channels and revisit the existing classifications in terms of external parameters, say those parameters which can be defined only in terms of the geometrical characteristics of the channel and of the amplitude and phase of the forcing tide. A conceptual framework similar to that of *Lanzoni and Seminara* [1998] is adopted. However, their approach requires the specification of a representative scale of flow velocity within the estuary (say, the order of magnitude of velocity at the mouth), which in general cannot be prescribed a priori, without choosing a specific class of estuary, since it depends on the channel response to a given tidal forcing. In our analysis we first determine the above scale as a function of external parameters within the context of a simplified framework that considers only two major factors, namely channel convergence and friction. Our estimate covers both the asymptotic cases of strongly convergent and strongly dissipative estuaries, for which the solution is already known [*Lanzoni and Seminara*, 1998]. Such scale is then compared with that obtained in closed form on the basis of the set of equations proposed by *Savenije and Veling* [2005].

It is worth noting that seeking a correct scale of velocity is a quite relevant issue since almost all the morphological processes in tidal channels depend on the order of magnitude of velocity. One may argue that the knowledge of the velocity scale at the mouth can only provide a rough indication of the hydrodynamic behavior, for which the full solution of the tidal motion within the entire channel would be required. In this respect, several attempts to produce such information, which mostly rely on analytical solutions, are available in the literature [e.g. *Lanzoni and Seminara*, 1998; *Friedrichs and Aubrey*, 1994; *Friedrichs et al.*, 1998; *Savenije*, 1993; *Savenije and Veling*, 2005]. However, we notice that the velocity scale at the mouth can provide a suitable description of the overall dynamics in terms of external parameters when the variation of velocity amplitude keeps relatively small along the channel. This applies to tidal channels whose hydrodynamic behavior falls within a neighbor of the marginal conditions for wave amplification, say those conditions for which the tidal amplitude does not grow (forced by channel convergence) nor decay (due to frictional dissipation) within a given reach. Field observations (e.g. *de Jong and Gerritsen* [1984] for the Western Scheldt) and the results presented in Section 7 seem to suggest that the above conditions are approximately met in several estuaries. Moreover, both observational evidences and theoretical results [*Myrick and Leopold*, 1963; *Savenije*, 1993; *Lanzoni and Seminara*, 2002; *Todeschini et al.*, 2003] indicate that the bed profile of tidal channels evolves towards a configuration which ensures a nearly constant velocity amplitude along the channel.

In the general case the information related to the velocity scale at the mouth must be coupled with a suitable description of the amplification process of the tidal wave. Then, as a second step in our analysis, we investigate the marginal conditions for tidal wave amplification. A first attempt to characterize the behavior of a tidal wave in convergent geometries is due to *Green* [1837], who deter-

mined the simple relationship

$$\frac{a(x)}{a_0} = \left(\frac{B_0}{B(x)}\right)^{1/2} \left(\frac{D_0}{D(x)}\right)^{1/4}, \qquad (1)$$

where a, B and D are the local values of tidal amplitude and of the width and depth of the channel, respectively (the subscript 0 denotes the values at the mouth). The Green's law relies on two unrealistic assumptions, namely that energy dissipation is negligible and convergence length is much longer than the tidal wavelength. In particular, the frictionless character of the solution does not allow one to describe the wave damping. According to (1) any degree of channel convergence or any decrease of the flow depth should result into an amplification of the tidal wave, which is obviously not true in real estuaries. Green's law has been recently revisited by many authors [*Jay*, 1991; *Friedrichs and Aubrey*, 1994; *Friedrichs et al.*, 1998; *Lanzoni and Seminara*, 1998; *Savenije*, 2001; *Savenije and Veling*, 2005] and the role of friction has been suitably included in the analysis.

In the present paper the amplification process of the tidal wave in convergent estuaries is investigated in terms of the same set of external parameters which are adopted to define the velocity scale. In particular, we try to emphasize the role of finite amplitude effects on tide propagation and the dependence of marginal conditions for wave amplification on the amplitude of the tidal wave. The latter effect has not received specific attention in previous works, since most of them tackle the problem of wave propagation in convergent estuaries by means of analytical models which are based on the assumption that the tidal amplitude a can be assumed to be small as compared with the tidally averaged depth D. In terms of the dimensionless tidal amplitude

$$\varepsilon = \frac{a_0}{D_0}, \qquad (2)$$

the above assumption reads

$$\varepsilon \ll 1. \qquad (3)$$

The assumption (3) allows for a linearization of the governing equations, leading to analytical solutions. However, the condition (3) is not always met in real estuaries, as shown in Table 1 where typical estimates of the amplitude ratio ε for some estuaries are given: data are based on the values reported by *Lanzoni and Seminara* [1998] and *Savenije* [2001].

More in general, we note that the role of non-linear terms may strongly influence the changes of tidal wave characteristics along the estuary, as it has been clearly recognized in previous analyses [e.g. *Parker*, 1991; *Le Provost*, 1991]. In particular, non-linear terms are able to produce higher harmonics, even when the system is forced by a simple sinusoidal tidal oscillation. In order to preserve the fully non-linear character of the governing system, in the present analysis we follow a numerical approach. A relatively simple model is used to investigate the role of different controlling parameters on the properties of the tidal wave, namely channel geometry, friction and tidal forcing. Hence, several simplifying assumptions are introduced: in particular, we ignore the presence of intertidal areas as well as the effect of the incoming river discharge.

The main output of the model is that the marginal conditions for tidal wave amplification in convergent estuaries, set in terms of the relevant dimensionless param-

eters accounting for the relative role of inertia, friction and convergence, may be strongly affected by the amplitude of tidal wave; as a result the analytical estimates based on linearized models are only obtained for small values of ε.

The rest of the paper is organized as follows. In the next section we introduce the mathematical model. The definition of the characteristic scales and of the relevant dimensionless parameters is given in Section 3, while a suitable evaluation of the dependent scales of velocity and length, set in terms of external variables, is given in Section 4. In Section 5 we derive the analytical solution of the set of the non-linear algebraic equations proposed by *Savenije and Veling* [2005] and we compare it with our analytical and numerical estimates. We then briefly revisit the subject of estuarine classification in terms of the above scales (Section 6) and we derive a relationship for the marginal conditions of tidal amplification in convergent estuaries (Section 7).

2. Formulation of the problem

We consider a tidal channel with varying width and depth and we investigate the propagation of the tidal wave within the framework of a one-dimensional cross-sectionally averaged model.

We assume that a rectangular cross-section is suitable to describe, as a first approximation, the behavior of a real section of the channel. Notice, however, that the choice of a triangular cross-section may have a significant influence as shown by *Prandle* [2003]. In order to reduce the number of the parameters involved in the problem, we also neglect the influence of the intertidal areas adjacent to the channel.

The sketch of the geometry of the idealized tidal channel is represented in Figure 1, where x is the longitudinal coordinate directed landward, starting from the mouth of the estuary. The standard one-dimensional shallow water equations are used, which read

$$\frac{\partial Q}{\partial t} + \frac{\partial}{\partial x}\left(\frac{Q^2}{\Omega}\right) + g\Omega\frac{\partial H}{\partial x} + g\Omega j = 0, \tag{4}$$

$$\frac{\partial \Omega}{\partial t} + \frac{\partial Q}{\partial x} = 0, \tag{5}$$

where t is time, Q is the water discharge, Ω is the area of the cross-section, H is the free surface elevation, g is gravity, D is the water depth and j is the friction term. The friction term reads

$$j = \frac{U\,|U|}{gC_h^2 R_h}, \tag{6}$$

where U is the cross-section averaged velocity, C_h is the dimensionless Chézy coefficient and R_h is the hydraulic radius. Following the practice to assign the Gauckler-Strickler coefficient k_s, we set $C_h = k_s R_h^{1/6}/\sqrt{g}$.

We assume that the width of the channel B can be described using an exponentially decreasing function

$$B(x) = B_\infty + (B_0 - B_\infty)\exp\left(-\frac{x}{L_b}\right), \tag{7}$$

where L_b is the convergence length. The asymptotic width B_∞ is included to set a minimum landward width when the estuary is long compared with L_b. Alternative choices with respect to (7) have been proposed to fit the real estuarine geometry, like power laws or more complex regressions [e.g. *Prandle*, 1991]. The exponential relation

(7) allows one to express the channel convergence in the simple form

$$\frac{1}{B}\frac{dB}{dx} = -\frac{1}{L_b}\frac{B - B_\infty}{B} = -\frac{1}{L_b}\,\psi_b, \tag{8}$$

where ψ_b is a function of B. When the asymptotic width B_∞ is much smaller than the actual width, ψ_b is nearly equal to 1, thus the dependence on the width can be ruled out from the governing equations. Finally, as a first approximation, the channel bottom is assumed to be horizontal.

The seaward boundary condition is given in terms of the free surface by the sea level, which is assumed to be determined by the tidal oscillation without any influence of the internal response of the estuary. Present analysis is restricted to a sinusoidal forcing

$$H = a_0 \sin\left(2\pi t/T_0\right), \tag{9}$$

with constant amplitude a_0, corresponding to an M_2 tide with a semidiurnal period T_0; hence we neglect external overtides and the monthly cycle of neap/spring tides.

The choice of a suitable landward boundary condition is not straightforward and depends on the characteristics of the estuary. Two extreme cases can be identified: the reflecting barrier and the transparent condition. The former situation corresponds to a closed boundary and implies vanishing discharge at the landward end of the channel, which determines the complete reflection of the wave. The latter condition refers to a tidal river; if the fluvial discharge is negligible, as we will assume in the following, the tidal wave exits from the computational domain without being deformed or reflected. It is worth mentioning that in the case of strongly convergent channels tide propagation is only weakly dependent on the choice of the landward boundary condition [*Friedrichs and Aubrey*, 1994].

The variables H and Q are obtained by the numerical solution of the system (4)-(5), discretized through finite differences and solved using the explicit McCormack method [see also *Lanzoni and Seminara*, 2002]. We note that the discharge Q is used instead of the velocity U in order to write the differential system in a more conservative form. The numerical method, provided the usual CFL condition is satisfied, is second order accurate both in space and in time. In order to avoid spurious oscillations, in particular when the wave steepens due to frictional or geometrical effects, a TVD filter is applied (see, for instance, *Garcia-Navarro et al.* [1992]). Numerical results presented in the following sections come from several hundreds of numerical simulations corresponding to different combinations of model parameters which cover a wide spectrum of tidal channels in nature.

3. External parameters

The hydrodynamic behavior of an estuary can be roughly characterized in terms of few dimensionless parameters, whose definition implies the introduction of suitable scales. In tidal systems the scale of velocity cannot be directly prescribed, since it results from the global response of the estuary to the forcing conditions. Moreover, different length scales can be defined, depending on the period of the forcing and the characteristics of the channel.

Several attempts to identify suitable scales (e.g., a simple scale for the velocity) and the governing parameters of tidal hydrodynamics can be found in the literature [e.g.

Jay, 1991; *Savenije*, 1993; *Friedrichs and Aubrey*, 1994; *Lanzoni and Seminara*, 1998; *Savenije and Veling*, 2005]. However, the above approaches are not entirely based on independent external parameters and thus the resulting estimates cannot be used as fully predictive tools. The need for characterizing tidal motion in terms of independent external parameters has not been clearly recognized until now. For instance, *Savenije* [1992, 2001] and *Savenije and Veling* [2005] propose a set of equations to describe the response of tidal channels to external forcing; however, their relationships are given in terms of parameters which are not known a priori unless the flow field is computed. In particular, their velocity scale is set in terms of the phase lag between high water and high water slack, though an analytical solution can be derived in terms of external parameters, as shown in Section 5.

In the following we essentially adopt the same set of parameters introduced by *Lanzoni and Seminara* [1998]. In their formulation the explicit evaluation of these parameters requires the introduction of an estuarine classification, since a suitable estimate of the scale of velocity must be supplemented, which in turn depends upon the dominant process governing the hydrodynamical response.

In the present work we pursue the attempt to define the relevant dimensionless parameters only in terms of external quantities, namely the tidal period T_0, the amplitude of tidal oscillation a_0, the reference values of channel width B_0 and depth D_0, evaluated at the mouth of the estuary, the characteristic length of width variations L_b and the reference value C_0 of the Chézy coefficient. The above parameters allows one to account for the basic ingredients of tidal hydrodynamics, namely friction, inertia and convergence. It is worth noting that the role of the channel length, which may become the dominant length in short channels where the tidal wave is reflected by the landward boundary, is not considered herein. However, the reflection can be damped by a landward shoaling bottom also in the case of a relatively short channel.

We express the a priori unknown scales of length L_0 and velocity U_0 in terms of the frictionless scales, L_g and U_g, in the form

$$\lambda = \frac{L_g}{L_0}, \qquad \mu = \frac{U_0}{U_g}, \tag{10}$$

where

$$L_g = \sqrt{gD_0}T_0, \tag{11}$$

and

$$U_g = \varepsilon\sqrt{gD_0} = \frac{a_0 L_g}{D_0 T_0}. \tag{12}$$

In the next section the coefficients λ and μ will be estimated in terms of external parameters.

A first relevant external parameter is the dimensionless tidal amplitude ε, which is defined as in (2). Further parameters can be obtained through equations (4) and (5). In particular, setting $\psi_b = 1$, momentum and continuity equations read

$$\frac{\partial U}{\partial t} + U\frac{\partial U}{\partial x} + g\frac{\partial H}{\partial x} + gj = 0\,, \tag{13}$$

$$\frac{\partial H}{\partial t} + D\frac{\partial U}{\partial x} + U\frac{\partial H}{\partial x} - U\frac{D}{L_b} = 0\,, \tag{14}$$

where the bed has been assumed to be fixed.

We introduce the following scaling:

$$D = D_0 D^*, \quad H = a_0 H^*, \quad U = \mu U_g U^*,$$
$$x = \frac{L_0}{2\pi} x^*, \quad t = \frac{T_0}{2\pi} t^*, \quad C_h = C_0 \mathcal{C}, \tag{15}$$

where an asterisk denotes dimensionless variables. Substituting from (6) into (13), with the assumption $R_h \simeq D$, the system (13)-(14) reads

$$\frac{\partial U^*}{\partial t^*} + \varepsilon\mu\lambda U^* \frac{\partial U^*}{\partial x^*} + \frac{\lambda}{\mu}\frac{\partial H^*}{\partial x^*} + \mu\chi \frac{U^* |U^*|}{\mathcal{C}^2 D^*} = 0\,, \tag{16}$$

$$\frac{\partial H^*}{\partial t^*} + \mu\lambda \left(D^* \frac{\partial U^*}{\partial x^*} + \varepsilon U^* \frac{\partial H^*}{\partial x^*} \right) - \mu\gamma U^* D^* = 0\,, \tag{17}$$

where the following dimensionless parameters arise:

$$\gamma = \frac{L_g}{2\pi\, L_b}\,, \tag{18}$$

$$\chi = \varepsilon \frac{L_g}{2\pi C_0^2\, D_0}\,. \tag{19}$$

The parameter γ (convergence ratio) accounts for the effect of width variation along the estuary, while the parameter χ is related to the ratio between friction and inertia. We note that the actual friction to inertia ratio is $\mu\chi$, as it can be clearly seen from (16), while $\mu\gamma$ measures the kinematic effect of channel convergence relative to the temporal oscillation of free surface elevation. In fact, both *Parker* [1991] and *Lanzoni and Seminara* [1998] set their estuarine classification in terms of the ratio R/S, where (in our notation) $R = U_0^2/(g\, C_0^2\, D_0)$ and $S = 2\pi U_0/(g\, T_0)$ account for the relative effect of friction and inertia with respect to gravity. As pointed out before, according to their formulation the velocity scale U_0 should be given a priori, while it can only be determined once the hydrodynamic field is known.

On the other hand, the external definition (19) does not require the knowledge of the scale of velocity: hence, the advantage with respect to the existing formulations is that γ and χ can be estimated directly on the basis of directly measurable quantities. Hence, a classification of estuaries based on external parameters can be introduced, set in terms of the friction to inertia ratio and of the convergence ratio

$$\frac{R}{S} = \mu\,(\chi, \gamma)\,\chi\,, \qquad K = \mu\,(\chi, \gamma)\,\gamma\,, \tag{20}$$

as in *Lanzoni and Seminara* [1998], provided we are able to establish a suitable relationship between the dimensionless scale of velocity μ and the parameters γ and χ. This problem is tackled in the next section.

Estimated values of the convergence length, Chézy coefficient and velocity scale for some estuaries are given in Table 1 along with the corresponding values of the dimensionless parameters χ and γ. The table is based on the data reported by *Lanzoni and Seminara* [1998] and by *Savenije* [2001]. As for the latter Author, values of the velocity scale are not included since they were not directly measured.

It is important to note that data reported in Table 1 highlight the strong correlation between the dimensionless parameters χ and ε, as it clearly emerges from Figure 2. In fact, given realistic values of depth and Chézy coefficient, the range of variation of χ is related to ε due to the linear dependence embodied in (19): large values of ε typically correspond to large values of χ. This fact will be further discussed in Section 7.

The correspondence between our parameters and those used in *Lanzoni and Seminara* [1998] is reported in Table 2.

4. The scale of velocity

We now attempt to derive a suitable reference scale of velocity in terms of external parameters, that is to relate the dimensionless scale μ to the parameters χ and γ characterizing the estuarine channel. Following the lead of *Lanzoni and Seminara* [1998], our analysis is based on dimensional arguments; moreover, the results of the numerical model are used to determine the relative importance of terms appearing in the governing equations and to check the suitability of our assumptions.

Before introducing a new velocity scale for the general case, we first revisit the results already obtained for two asymptotic cases [*Lanzoni and Seminara*, 1998], and test their range of applicability through a comparison with the results of the fully non-linear numerical model. It is important to note that as a numerical estimate of the scale of velocity, U_0, we use the algebraic mean of the absolute values of flood and ebb peaks of velocity evaluated at the mouth of the estuary.

We now consider the first of the two asymptotic cases. In the strongly convergent and weakly dissipative case (large values of γ and small values of χ), the continuity equation (17) reduces to a balance between the inertial term $\partial H^*/\partial t^*$ and the convergence term $\mu\gamma U^* D^*$, which implies:

$$\mu\gamma \sim 1. \tag{21}$$

Hence, the dimensionless velocity scale can be given the following estimate [*Lanzoni and Seminara*, 1998]:

$$\mu \sim \frac{1}{\gamma}. \tag{22}$$

In Figure 3 we test the above estimate against the numerical results: it appears that equation (22) is strictly valid only for large values of γ (say $\gamma > 3$, strongly convergent estuaries), for which the influence of χ is negligible. We note that, for given values of the depth D_0, the dependence on the parameter χ is felt through the parameter ε. The curve corresponding to $\varepsilon = 0.001$ displays an oscillating behavior which may be due to amplification associated with the transition through the condition of critical convergence, as defined by *Jay* [1991]. An improvement of equation (22) can be obtained if we consider that the value $\gamma = 2/\pi$ (for which L_b is a quarter of the frictionless wavelength L_g) corresponds to the lower limit for strong convergence (see also *Jay* [1991] and *Lanzoni and Seminara* [1998]). For $\gamma > 2/\pi$, the velocity scale is better fitted through the following estimate

$$\mu \sim \frac{1}{\gamma - 2/\pi}, \tag{23}$$

whose adaptation to numerical results is more satisfactory in the weak dissipation limit $\varepsilon \ll 1$, which corresponds to $\chi \ll 1$.

The dimensionless length scale λ, defined in equation (10), can be obtained through the momentum equation (16), which essentially reduces to a balance between local inertia $\partial U^*/\partial t^*$ and gravity $\lambda/\mu\, \partial H^*/\partial x^*$ and implies $\lambda \sim \mu$. Using relationship (22), the dimensional length scale can be given the form $L_0 \sim \gamma L_g$. Note that L_0, which is a measure of the longitudinal variations, may

be much longer than the convergence length, as can be readily derived using definition (18). We observe that in this case the tidal wave tends to lose its dependence on the reflected wave at the landward boundary [*Friedrichs and Aubrey*, 1994].

The other asymptotic case, the strongly dissipative and weakly convergent limit (large χ, small γ), can be examined using the same procedure adopted in the previous case [see also *Lanzoni and Seminara*, 1998]. When γ is negligible, the continuity equation (17) implies a balance between two terms, namely $\partial H^*/\partial t^*$ and $\mu\lambda\, D^*\partial U^*/\partial x^*$. In this case the velocity scale cannot be directly determined from continuity equation since the length scale λ is also unknown. Hence, the momentum equation (16) is required for its evaluation.

Assuming that the term $\epsilon\mu\lambda U^*\partial U^*/\partial x^*$ is always negligible, the relative importance of the remaining terms changes during the tidal cycle. Since the aim of the analysis is to determine a reference value of velocity corresponding to its peak values, here we consider those parts of the tidal cycle in which the velocity is around its maximum value. Under these conditions the local inertia $\partial U^*/\partial t^*$ vanishes, letting the frictional term $\mu\chi U^*\,|U^*|\,/\left(\mathcal{C}^2 D^*\right)$ and the gravitational term $\lambda/\mu\partial H^*/\partial x^*$ to balance. We note that, on the contrary, as the velocity vanishes friction is no longer dominant and a balance between gravity and inertia holds.

As a result, continuity and momentum equations suggest that in the strongly dissipative and weakly convergent limit the following relationships hold

$$\mu\lambda \sim 1, \qquad \frac{\lambda}{\mu} \sim \mu\chi, \tag{24}$$

which imply

$$\mu \sim \chi^{-1/3}, \qquad \lambda \sim \frac{1}{\mu}. \tag{25}$$

Note that in constant-width channels the dimensionless velocity depends only on χ and does not depend directly on ε. The estimate (25) is fairly well reproduced by the numerical results, as reported in Figure 4: the agreement is satisfactory for $\chi > 2$. For $\chi < 1$ the above solution does not hold: in this case equation (25) would lead to $\mu > 1$, which is not possible because $\mu = 1$ is the upper limit for the frictionless case (unless resonant phenomena are considered, which can occur in short channels).

At this point we can consider the general case, for those estuaries that are characterized by values of the parameters γ and χ such that both friction and convergence are important; note that this is the most common case. Building upon the results obtained previously, we propose a novel formulation to evaluate the reference velocity at the mouth of the estuary in terms of external parameters, when both χ and γ are not vanishing. For the momentum equation (16), the same balance as in the strongly dissipative and weakly convergent asymptotic case holds. On the other hand, in the continuity equation (17) the time derivative $\partial H^*/\partial t^*$ balances both $\mu\lambda\, D^*\partial U^*/\partial x^*$ and $\mu\gamma U^* D^*$. Thus, we can generalize (21) and (24) in the following form:

$$\mu\lambda + \mu\gamma \sim 1, \qquad \frac{\lambda}{\mu} \sim \mu\chi, \tag{26}$$

where the former relationship covers both the asymptotic cases discussed above, as χ or γ vanishes.

The above estimates on the relative importance of various terms in the governing equations are confirmed by

the results of numerical simulations; an example is given in Figure 5 where the time variation of different terms appearing in the dimensional equations (13) and (14) is reported for a dissipative and convergent channel. In the plot we suggest to focus the attention on those parts of the tidal cycle in which the velocity attains its maximum in absolute value, which are determined according to the results reported in Figure 6.

From (26), simple algebraic manipulations lead to the following dimensionless relationship

$$\mu\left(\gamma + \mu^2 \chi\right) = 1, \tag{27}$$

which can be cast in the following form

$$\mu(\chi, \gamma) = \frac{1}{\widehat{\chi}}\left(\Delta - \frac{1}{\Delta}\frac{\widehat{\gamma}}{\widehat{\chi}}\right), \tag{28}$$

where we have set

$$\Delta = \left[1 + \sqrt{1 + \left(\frac{\widehat{\gamma}}{\widehat{\chi}}\right)^3}\right]^{\frac{1}{3}}, \ \widehat{\chi} = (2\chi)^{1/3}, \ \widehat{\gamma} = \max\left[0, \frac{2}{3}(\gamma - \frac{2}{\pi})\right]. \tag{29}$$

Note that a modified parameter $\widehat{\gamma}$ has been suitably introduced, with the subtraction of $2/\pi$ on the basis of the considerations reported in deriving equation (23). The relationship (28) is valid provided the frictionless limit $\mu \leq 1$ is satisfied and for constant-depth channels which are long enough to be unaffected by the influence of the landward boundary condition.

Finally, according to (26), the characteristic length scale can be expressed in terms of the solution (28) in the following form

$$\lambda = \chi\, \mu^2(\chi, \gamma), \tag{30}$$

which is valid only when χ does not vanishes.

In Figure 7 the proposed analytical scale for velocity (solid lines) is compared with the results of numerical simulations (broken lines). Numerical results correspond to different values of ε, which ranges between 0.1 and 0.3: this allows us to cover a relatively wide range of values of χ while keeping the friction coefficient within a realistic range of values (in the numerical simulations we use different values of Gauckler-Strickler coefficient k_s). In fact, for a given ε numerical results can cover only a restricted range of values of χ, which changes for different values of D_0.

The agreement between the theoretical formulation (28) and numerical results is fairly satisfactory within a wide range of values of the governing parameters. We may observe that the dimensionless amplitude ε does not seem to influence the numerical solution. The discrepancy between theoretical estimate and numerical results is larger for weakly dissipative and weakly convergent estuaries. However, in these cases the frictionless scale (12) provides a suitable estimate of the order of magnitude of velocity.

We now try to test the relationship (28) using the available data on the velocity scale U_0 measured in some estuaries, which are summarized in Table 1. The comparison between estimated and observed values of reference velocity is given in Figure 8: the agreement seems fairly satisfactory, given the over-simplified one-dimensional geometrical schematization adopted in our model and the uncertainties affecting measured data. For instance, in

the case of the Scheldt estuary, the maximum velocity at the mouth of the estuary is actually around $1\,m/s$ [*Toffolon*, 2002], while the value $0.5\,m/s$ reported by *Lanzoni and Seminara* [1998] refers to the tidally averaged velocity evaluated using tidal volumes by *de Jong and Gerritsen* [1984]. We note also that, since no information is provided about the presence of tidal weir which may affect the landward boundary condition, the effect of the finite length of the estuary is not included in the analysis.

5. The analytical solution of Savenije's model

In this section we revisit the analytical approach proposed by *Savenije* [1992, 1993, 1998, 2001, 2005] and *Savenije and Veling* [2005] in terms of the external parameters χ, γ and ε adopted in the present work. In particular, we show that from their set of equations an estimate of the velocity scale can be derived in closed form and we test their prediction against the fully numerical solution of the problem. In the following we refer to the set of equations reported in *Savenije and Veling* [2005], where an analytical system of four equations is proposed in terms of tidal velocity amplitude, tidal wavelength, damping length scale (δ_H or δ_u, see below) and phase lag α between high water and high water slack ($\alpha = 0$ for a standing wave and $\alpha = \pi/2$ for a progressive one).

We rewrite the Authors' relationships in our notation (see Table 3) neglecting the presence of intertidal areas. We also introduce the dimensionless tidal damping

$$\delta = \frac{L_g}{2\pi}\delta_H \simeq \frac{L_g}{2\pi}\delta_u \,, \tag{31}$$

where we follow the same approximation proposed by*Savenije* [1993, 2001]. Since we are mainly concerned with the scale of velocity at the mouth, we specify the governing system at $x = 0$ (see also Table 3). The damping equation (eq. 34 in *Savenije and Veling*, 2005), the scaling equation (eq. 16) for tidal velocity amplitude, the celerity equation (eq. 33) and the phase lag equation (eq. 15) take the following form

$$\delta\left(1 + \frac{\lambda}{\mu \sin\alpha}\right) = \gamma - \mu\chi\lambda\sin\alpha \,, \tag{32}$$

$$\mu = \frac{\sin\alpha}{\lambda} \,, \tag{33}$$

$$\lambda^2 = 1 - \frac{\delta\cos\alpha}{\mu} \,, \tag{34}$$

$$\tan\alpha = \frac{\lambda}{\gamma - \delta} \,, \tag{35}$$

where the actual celerity has been expressed as $c = c_0/\lambda$. The above system constrains the solution space of the unknown variables μ, λ, δ and α. We note that it has been derived under the assumption of small values of dimensionless tidal amplitude ε.

Algebraic manipulation of (32), (33), (34) and (35) allows us to find the solution for tidal velocity amplitude μ in the form of a 10-th order equation, which involves three families of solutions. One of them, namely $\mu^2+\gamma\mu+1 = 0$, must be discarded because it gives only negative values of μ. The second family,

$$\mu^2 - \gamma\mu + 1 = 0 \,, \tag{36}$$

only depends on γ; its solution reads

$$\mu = \frac{\gamma}{2} - \frac{1}{2}\sqrt{\gamma^2 - 4}\,, \tag{37}$$

which attains real values only for $\gamma > 2$. The third family,

$$\mu^6\chi^2 + \mu^4\chi\gamma + 2\mu^2 - 2 = 0\,, \tag{38}$$

can be solved to give the real solution

$$\mu = \sqrt{\frac{1}{3\chi}\left[\widetilde{\Delta} + \frac{(\gamma^2 - 6)}{\widetilde{\Delta}} - \gamma\right]}\,, \tag{39}$$

where

$$\widetilde{\Delta} = \left[27\chi + \gamma\left(9 - \gamma^2\right) + 3\sqrt{3\chi\left[27\chi + 2\gamma\left(9 - \gamma^2\right)\right] + 3\left(8 - \gamma^2\right)}\right]^{1/3}\,. \tag{40}$$

One may argue that equation (39) is the physical solution of the problem, inasmuch as it depends both on χ and γ; however, the above conclusion is not always correct, as shown below.

Once the solution for μ is obtained, the other unknowns can be computed as

$$\delta = \mu^2\frac{(\gamma^2 - 1)\chi\mu^2 + 2\gamma - \chi}{\mu^4\chi\gamma + 2\mu^2 + 2}\,, \tag{41}$$

$$\cos(\alpha) = \mu\frac{2\gamma + \mu^4\chi + \chi\mu^2}{\mu^4\chi\gamma + 2\mu^2 + 2}\,, \tag{42}$$

$$\lambda^2 = \frac{(\mu^2 + \gamma\mu + 1)(\mu^2 - \gamma\mu + 1)(\chi^2\mu^4 + 2\chi\mu^2\gamma + 4)}{(\mu^4\chi\gamma + 2\mu^2 + 2)^2}\,. \tag{43}$$

A careful inspection of solutions (41), (42), (43) is required in order to choose the physical solution for μ between (37) and (39). In particular, equation (41) suggests that increasing γ implies a transition from negative values of δ (damping) to positive values (amplification). On the other hand, equation (43) gives real values of λ provided

$$\mu^2 - \gamma\mu + 1 \geq 0\,. \tag{44}$$

It is easy to show that solution (37) automatically satisfies this condition within its range of validity ($\gamma > 2$). On the contrary, solution (39) conforms to (44) within a region of the χ-γ plane delimited by a threshold curve $\gamma_{cr}(\chi)$. In fact, for $\gamma > \gamma_{cr}$ the solution (39) is not physical because (43) would imply an imaginary wavelength; hence, the threshold curve marks the transition to the other solution (37). We note that (37), which depends only on γ, corresponds to the solution valid in the strongly convergent limit, when the dependence on χ is negligible; in this case (43) gives $\lambda = 0$, which implies that the wavelength $L_0 \to \infty$ [*Friedrichs and Aubrey*, 1994].

The comparison between the analytical solution of the system (32-35) and the relationship (28) is plotted on the χ-γ plane in Figure 9 (the corresponding numerical results are given in Figure 7). The analytical relationships are tested against the results of the fully numerical model on the parity diagram of Figure 10. We can see that both solutions behave reasonably well; in particular, (28) performs satisfactorily when finite amplitude effects are significant, say for μ smaller than about 0.7. As already noted in Section 4, such scale fails for $\mu \to 1$, where models based on the assumption of small tidal amplitude,

like (37)-(39), provide better estimates.

6. Estuarine classification

Various attempts to characterize the hydrodynamic response of estuaries, based on the values of dimensionless parameters, can be found in the literature (see, among others, the classification introduced by *Lanzoni and Seminara* [1998] in terms of weakly/strongly convergent and weakly/strongly dissipative tidal channels). We now try to revisit the subject in the light of the results of present work and test in which cases the scale of velocity (28), which accounts for both convergence and friction, has to be applied. This will also enable us to assess the range of validity of the asymptotic solutions. We base our classification on the external parameters γ and χ defined in Section 3. As discussed above, the relative importance of friction with respect to inertia is measured by the product $\mu\chi$, where μ is dependent on both χ and γ as shown in Figure 7.

In the strongly convergent and weakly dissipative limit, negligibility of frictional term $\mu\chi U^* |U^*| / \left(\mathcal{C}^2 D^*\right)$ with respect to gravitational $(\lambda/\mu)(\partial H^*/\partial x^*)$ and inertial $(\partial U^*/\partial t^*)$ terms in momentum equation (16) requires that

$$\chi \ll \gamma \,, \tag{45}$$

where the asymptotic relationships for μ and λ, derived in the corresponding case of Section 4, have been used. Given the condition (45), also the balance (21) adopted in the continuity equation (17) is justified. Note that a strongly convergent channel keeps weakly dissipative also for relatively large value of χ. This can be easily explained if we consider that μ decreases when γ and χ increase, so that the product $\mu\chi$ keeps limited.

Actually, the real condition which distinguishes the weakly dissipative case can be obtained using the general scale (28) for μ in the condition $\mu\chi \ll 1$. The curve $\mu\chi = 1$ is plotted in Figure 11, where the regions of validity of the condition (45) and of the condition corresponding to the strongly dissipative limit (see below equation 46) are also indicated. We may note that the general condition $\mu\chi = 1$ is well fitted by the curve $\gamma = \chi$. It is worth recalling that, according to previous analysis, the definition of the friction to inertia ratio requires the knowledge of the velocity scale from field measurements, while in the present formulation the validity limits of the asymptotic relationships can be given in the χ-γ plane, that is in terms of external parameters.

The other asymptotic case is the weakly convergent and strongly dissipative limit. The convergence term $(\mu\gamma U^* D^*)$ in the continuity equation (17) can be neglected with respect to $(\partial H^*/\partial t^*)$ and $(\mu\lambda\, D^* \partial U^*/\partial x^*)$ provided the following condition holds:

$$\gamma \ll \chi^{1/3} \,, \tag{46}$$

which can be readily derived by substituting the relationships (25) in the conditions $\mu\gamma \ll 1$ or $\mu\gamma \ll \mu\lambda$.

The general solution (28) is plotted in Figure 12 along with the contour lines of the friction to inertia ratio $\mu\chi$: in the limits $\gamma \ll 1$ or $\chi \ll 1$ the dependence on the parameters χ and γ vanishes, respectively. It appears that most of the data from real estuaries reported in Table 1 fall within the region laying between the conditions (45) and (46), where the simplified asymptotic solutions do not hold. Finally, we note that the contour line $\mu = 1$ lays close to the boundary of the region $\gamma < 1$ and $\chi < 1$,

where the frictionless solution is approximately valid.

As pointed out in Section 3, the short channel limit is not discussed herein. The case is relevant when a reflective barrier is imposed at the landward end such that the length scale of frictional damping is larger than the physical length. Under this condition the description of the tidal wave can be greatly simplified, as shown, for instance, by *Ippen* [1966] and *Schuttelaars and de Swart* [1999]. In this case the length scale for the variation of velocity coincides with the physical length of the estuary and the velocity follows approximately a linear behavior along the estuary; furthermore, the length scale of free surface oscillation increases as the channel length decreases.

7. Marginal conditions for amplification

The dynamic balance which governs the amplification of a tidal wave in estuarine channels essentially involves convergence and friction: in our analysis these effects are described in terms of the dimensionless parameters γ and χ, respectively. In this section we study the marginal conditions for the amplification of the wave amplitude; they are determined by those values of the above parameters for which the tidal wave does not amplify nor decay during its propagation, with respect to the high water level, within a convenient reach of the estuary relatively close to its mouth.

As pointed out in the Introduction, most of the analytical approaches which has been introduced so far to investigate the marginal conditions are based on the assumption that the parameter ε is relatively small. The resulting relationships for the marginal state can be cast in the following form:

$$\gamma = k\chi^m \,. \tag{47}$$

For weakly convergent and weakly dissipative estuaries *Lanzoni and Seminara* [1998] have obtained a linear dependence, with m=1 and $k = 8/(3\pi) \simeq 0.85$. On the other hand, for strongly convergent channels, *Friedrichs and Aubrey* [1994] have found that marginal conditions are attained when the actual celerity c of the tidal wave is equal to the frictionless value of celerity c_0. Adapting their relationship to our notation, we find in this case $m = 0.5$ and $k = \sqrt{8/(3\pi)} \simeq 0.92$.

However, according to field data reported in Table 1 the small-amplitude condition is rarely satisfied by real estuaries. The question then arises on whether the above marginal conditions are affected by the amplitude of the tidal wave. Here we try to address the above question through the numerical solution of the fully non-linear governing system.

The marginal conditions for tide amplification are determined through numerical experiments, running each simulation until a tidally averaged equilibrium state is reached by the system. Then, the resulting high water level at a given section is compared with that imposed at the mouth. The test section is chosen at a distance of nearly 60 km from the mouth: we note that a different choice does not affect the results significantly. An iterative algorithm is used in order to obtain, within a given tolerance, the value of the length L_b for which the difference between the two high water levels is minimized. Simulations are performed placing a reflective barrier at the landward end; however, the length of the estuary is always set as large enough to avoid any influence of the boundary condition on the solution.

The data set used for the determination of the

marginal conditions covers a wide range of values of the parameters, namely $D_0 \in [2.5\,m \div 50\,m]$, $\varepsilon \in [0.005 \div 0.6]$, $C_0 \in [10 \div 30]$, which are selected paying particular attention to the choice of typical conditions of real estuaries. To reduce the number of external parameters the channel is assumed to be wide and we set B_∞=0 and $R_h \simeq D$.

The marginal conditions obtained numerically are plotted in Figure 13 in terms of the dimensionless parameters χ and γ, for different values of the amplitude ratio ε. The region falling below the numerical points corresponds to wave damping during its propagation landward, while the region above them corresponds to wave amplification. The results clearly suggest that the larger are the dissipative effects along the estuary (large χ), the stronger is the degree of convergence required to achieve the marginal conditions. On the contrary, a relatively weak variation of channel geometry is able to produce the amplification of the tidal wave in weakly dissipative estuaries.

Figure 13 shows that numerical points corresponding to a given value of ε can be fitted fairly well through power law curves of the form (47), whose coefficients m and k depend on the parameter ε. The above dependence embodies the effect of the amplitude of the tidal wave on its amplification. The numerical findings are summarized in Figure 14 where m and k are plotted as functions of ε. It appears that the exponent m depends strongly on the amplitude ratio: its value decreases sharply as ε increases and reaches an almost constant value, nearly equal to 0.6, for relatively large values of ε.

The marginal curves reported in Figure 13 confirm the close relationship between the value of the dimensionless amplitude ε and the corresponding range of variation of the frictional parameter χ shown in Figure 2. Moreover, in the region of the χ-γ plane where the marginal curves are located, increasing χ results directly in a larger friction to inertia ratio $\mu\chi$ (see Figure 12).

Now, let us consider separately the two cases of weak and strong dissipation. Numerical results for the case of weakly convergent and weakly dissipative channels are represented by the curve corresponding to small values of ε in Figure 13. As pointed out before, the analytical solution suggests that in this case a linear relationship should hold, with m=1 and $k \simeq 0.85$. Results of numerical model conform to this behavior only for very small values of ε, which is consistent with the assumption ($\varepsilon \ll 1$, $\chi \ll 1$, $\gamma \ll 1$) under which *Lanzoni and Seminara* [1998] derived their solution. For commonly observed values of the tidal range within this class of estuaries (see Table 1) the power law is strongly non-linear as shown in the figure. This is also confirmed by the results reported in Figure 14 which show that the tendency of m towards unity as ε vanishes is almost vertical. The above findings suggest that the range of validity of the weakly dissipative linearized theories is quite limited since the fully non-linear solution diverges rapidly as ε increases. Also notice that the effect of the landward boundary condition becomes increasingly important in the numerical model as we approach the frictionless limit, that is for very small values of the dimensionless parameters χ and ε.

In the case of strong convergence and dissipation a significant influence of the tidal amplitude on wave characteristics can be expected along with a substantial deviation from the linear behavior. In this case the approximate analytical solution [*Friedrichs and Aubrey*, 1994] leads to a value of the exponent m =0.5 which is fairly close to the numerical result ($m \simeq 0.6$) within a wide range of values of ε, namely those which are typically en-

countered in real estuaries according to the data reported in Table 1. However, the coefficient $k \simeq 0.92$ of the analytical solution is attained by the numerical solution only in the case of $\varepsilon \to 0$ (see Figure 14), which is not typical of strongly convergent estuaries.

It is worth noting that in Figure 13 the marginal conditions for strongly dissipative channels are typically identified by relatively large values of ε, while γ keeps relatively close to unity (the marginal curves lay in the neighborhood of the $\gamma = \chi^{1/3}$ line which discriminates the weakly convergent case). On the other hand, the asymptotic solution of *Friedrichs and Aubrey* [1994] is based on two assumptions: strong convergence and values of ε small enough to linearize the equations. Since both approximations are not strictly verified in this case, this may explain the discrepancy between the fully non-linear numerical results and their analytical solution. Moreover, linearization of the friction term (6) is justified only for relatively short channels, in which non-linear effects cannot fully develop [*Lanzoni and Seminara*, 1998].

The marginal conditions for tidal wave amplification can be cast in a more suitable form if we introduce a modified parameter

$$\chi_\varepsilon = k(\varepsilon)\chi^{m(\varepsilon)}, \tag{48}$$

using the values of the coefficients k and m given in Figure 14. In this case the threshold lines discriminating amplification or damping of tidal wave collapse on a single curve $\gamma = \chi_\varepsilon$, as shown in Figure 15. In the same figure data from real estuaries taken from Table 1 are also reported. In the plot triangles denote those estuaries for which experimental evidence of wave amplification has been reported [*Ippen*, 1966; *Friedrichs and Aubrey*, 1994; *Savenije*, 2001], while squares indicate estuaries where tidal damping has been measured [*Savenije*, 2001]; for the remaining cases (circles) we were not able to find suitable information on wave behavior. In spite of the uncertainties affecting field data and of the approximations adopted in the present approach, the theory seems able to reproduce fairly well the overall behavior of the examined estuaries. The figure also suggests that a significant part of the estuaries considered in the analysis fall within a neighbor of the marginal conditions, which implies weakly amplifying waves. In these cases the estimated value of the velocity scale at the mouth obtained in Section 4 is more likely to provide a representative measure of the velocity scale within the whole estuary.

It is worth recalling that the suitability of the linear solution to reproduce measured data on wave amplification has been verified by *Friedrichs and Aubrey* [1994] for some estuaries; however, in their analysis a suitable choice of model parameters is introduced, whose values change along the estuary (two reaches are considered for Thames and three for Delaware). Close to the marginal state a significant departure of approximate linear solutions from the fully non-linear solution can be expected. This is confirmed by the comparison reported in Figure 16, where the marginal conditions obtained according to the analytical solutions of *Lanzoni and Seminara* [1998] and *Friedrichs and Aubrey* [1994] are tested against the same set of data. As pointed out before the main reason for the above discrepancy is related to fact that linearization is not justified, even under weakly amplifying (or damped) conditions, due to the strongly non-linear dependence of the solution on tidal amplitude, unless the amplitude ratio is vanishingly small.

Savenije [2001] proposes an alternative relationship for the marginal conditions, based on the criterion that the

actual wave celerity must equal the frictionless celerity, as in *Friedrichs and Aubrey* [1994]. The above criterion can be readily obtained from (34), which reduces to $\lambda = 1$ under marginal conditions ($\delta = 0$). Furthermore, under these conditions equations (32), (33) and (35) take the following form

$$\gamma = \mu\chi \sin\alpha\,, \quad \mu = \sin\alpha\,, \quad \tan\alpha = 1/\gamma\,. \tag{49}$$

Hence, the marginal conditions, as obtained through the model of *Savenije and Veling* [2005], can be given the following representation in terms of external parameters

$$\chi = \gamma(\gamma^2 + 1)\,. \tag{50}$$

The above relationship is tested against the results of the complete numerical solution in Figure 16. It appears that equation (50) is more accurate than the asymptotic solutions of *Lanzoni and Seminara* [1998] and *Friedrichs and Aubrey* [1994], though it departs from the complete solution as ε increases.

8. Conclusions

In this paper we have tackled the problem of defining the relevant dimensionless parameters which govern estuarine hydrodynamics in terms of externally defined quantities, namely the large-scale geometrical properties of the estuary and the characteristics of the tidal forcing. Motivation for the study comes from the recognition that the knowledge of the relationships between the hydrodynamic response of tidal channels and the external factors (length of the estuary, friction, channel convergence, bed altimetry, river discharge) is required to properly evaluate the consequence of both natural and anthropogenic modifications.

Despite the large number of contributions which have been devoted to the subject, these relationships are not clearly interpreted yet. Differently from previous authors, we have considered the scale of velocity as fully determined by the above parameters. Thus, without choosing a priori a class of estuary, we have introduced a classification based on the frictional parameter χ, defined in (19), and the convergence degree γ, given by (18). Using these parameters we have obtained a suitable scale of velocity μ, which covers both the case of strongly convergent and of strongly dissipative estuaries, and we have proposed an external definition of the ratio between friction and inertia (i.e. R/S, according to *Lanzoni and Seminara*'s [1998] notation) on which the existing criteria for estuarine classification are based. The agreement between the proposed estimate and the available data from real estuary is reasonable, given the strongly simplified character of the model and the uncertainty affecting literature data. Incidentally we notice that detailed field measurements of cross-sectional velocity, which can be obtained, for instance, through ADCP techniques, would be highly desirable in order to accurately verify the theoretical predictions.

We have shown that both friction and convergence tend to decrease the reference velocity with respect to its frictionless value ($\mu < 1$); on the other hand, convergence increases the characteristic length scale while friction tends to decrease it. We have also shown that marginal conditions for tidal wave amplification can be given the form of power laws in terms of the relevant dimensionless parameters which account for the effect of friction, inertia and convergence. Such laws exhibit a strong dependence on the dimensionless tidal amplitude

ε such that the linear behavior predicted by the analytical solution of *Lanzoni and Seminara* [1998] in the case of weakly dissipative and weakly convergent estuaries is recovered only for very small values of ε, while the strongly convergent solution of *Friedrichs and Aubrey* [1994] is not attained precisely.

Furthermore, we have tested against numerical results the analytical model proposed by *Savenije and Veling* [2005] [see also *Savenije*, 1992, 1993, 1998, 2001, 2005]. In particular, we have shown that the system of equations of *Savenije and Veling* [2005] can be solved in closed form, such that both an estimate of the velocity scale and the relationship for the marginal conditions can be obtained in terms of the external variables adopted herein. However, the analytical procedure is quite complex since it involves two different families of solutions. Moreover, as one may expect, the correspondence with numerical results is reasonable mainly for values of μ close to unity. In this respect, the scale (28), which has been derived on the basis of dimensional arguments, is simpler and seems more accurate for a larger set of parameters.

Finally, it is worth noticing that the geometry of the tidal channel has been strongly simplified in the present analysis, which essentially retains only the effect of the variable width. Some of the neglected aspects may turn out to be relevant, namely the effect of the incoming river discharge, depth variations and intertidal areas. The inclusion of such elements in a simplified model, like the one proposed here, would require a suitable schematization. The identification of a more realistic geometry, albeit simplified, through the definition of a macro-scale shape of the estuarine section, might constitute a step towards a better description of the natural systems. However, a one-dimensional model can hardly include relevant factors like the influence of the width to depth ratio (which crucially affects the bed response as shown by *Seminara and Tubino* [2001]), the behavior of the residual currents and the formation of morphological cells. More in general, the model adopted herein is unable to describe the role of two-dimensional effects which are relevant when the width of the channels is large enough to be comparable with the other scales (like, for instance, the convergence length in the seaward part of some strongly convergent estuaries). An attempt to define a nested model which might be able to consider feed-back mechanisms among different scales is currently under investigation. Within the above framework, the development of more refined two or three-dimensional models able to reproduce the formation of bar forms within a local approach (like those recently proposed by *Hibma et al.* [2003]) and to investigate the stability of the complex system of ebb and flood channels (like those described for instance by *Winterwerp et al.* [2001]) would be highly desirable.

Acknowledgments. The present work has been funded by the University of Trento and the Italian Ministry of Education, University and Research (MIUR) under the National program "Idrodinamica e morfodinamica di ambienti a marea" (Cofin 2002). We gratefully acknowledge the contribution of the reviewers, H. H. G. Savenije and S. Lanzoni, for their constructive criticism and various remarks that have stimulated a substantial improvement the original manuscript.

References

De Jong, H., and F. Gerritsen (1984), Stability parameters of Western Sheldt estuary, in *Proceedings of the 19th Coastal Engineering Conference*, edited by B. L. Edge, pp. 3078-3093, ASCE.

Dronkers, J. J. (1964), *Tidal Computations in River and Coastal Waters*, 518 pp., North-Holland, New Work.

Friedrichs, C. T., and D. Aubrey (1994), Tidal propagation in strongly convergent channels, *J. Geophys. Res., 99*, 3321-3336.

Friedrichs, C. T., B. D. Armbrust and H. E. de Swart (1998), Hydrodynamics and equilibrium sediment dynamics of shallow, funnel-shaped tidal estuaries, in *Physics of Estuaries and Coastal Seas*, edited by Dronkers and Scheffers, pp. 315-327, Balkema, Rotterdam.

Garcia-Navarro, P., F. Alcrudo and J. M. Saviron (1992), 1D open-channel flow simulation using TVD-McCormack scheme, *J. Hydraul. Eng., ASCE, 118*(10), 1359-1372.

Green, G. (1837), On the motion of waves in a variable canal of small depth width, *Trans. Cambridge Philos. Soc., 6*, 457.

Hibma, A., H. M. Schuttelaars and H. J. de Vriend (2003), Initial formation and evolution of channels-shoals patterns in estuaries, in *Proceedings of 3rd IAHR Symposium on River, Coastal and Estuarine Morphodynamics*, vol. 2, pp. 749-760, Barcelona (Spain).

Ippen, A. T. (1966), *Estuary and coastline hydrodynamics*, McGraw-Hill, New York.

Jarret, J. T. (1976), Tidal prism-inlet area relationship, in *Gen. Invest. Tidal Inlets, Rep. 3*, U.S. Army Corps Coastal Eng. Res. Center, Vicksburg, Miss.

Jay, D. A. (1991), Green's law revisited: Tidal long-wave propagation in channels with strong topography, *J. Geophys. Res., 96*(C11), 20585-20598.

Lanzoni, S., and G. Seminara (1998), On tide propagation in convergent estuaries, *J. Geophys. Res., 103*(C13), 30793-30812.

Lanzoni, S., and G. Seminara (2002), Long term evolution and morphodynamic equilibrium of tidal channels, *J. Geophys. Res., 107*, 1-13.

Le Provost, C. (1991), Generation of overtides and compound tides, in *Tidal hydrodynamics*, edited by B. B. Parker, pp. 269-297, John Wiley & Sons.

Myrick, R.M., and L.B. Leopold (1963), Hydraulic geometry of a small tidal estuary, *US Geological Survey Professional Paper 422-B*.

Parker, B. B. (1991), The relative importance of the various nonlinear mechanisms in a wide range of tidal interactions, in *Tidal hydrodynamics*, edited by B. B. Parker, pp. 237-268, John Wiley & Sons.

Prandle, D. (1991), Tides in estuaries and embayments, in *Tidal hydrodynamics*, edited by B. B. Parker, pp. 125-152, John Wiley & Sons.

Prandle, D. (2003), Relationships between tidal dynamics and bathymetry in strongly convergent estuaries, *J. Physical Oceanography, 23*(12), 2738-2750.

Prandle, D., and N. L. Crookshank (1974), Numerical Model of St. Lawrence River Estuary, *J. Hydraulics Division, ASCE, 100*(HY4), 517-529.

Savenije, H. H. G. (1992), Lagrangean solution of St. Venant's equations for an alluvial estuary, *J. Hydraul. Eng., ASCE, 118*(8), 1153-1163.

Savenije, H. H. G. (1993), Determination of estuary parameters on basis of lagrangian analysis, *J. Hydraul. Eng., ASCE, 119*(5), 628-642.

Savenije, H. H. G. (1998), Analytical expression for tidal damping in alluvial estuaries, *J. Hydraul. Eng., ASCE, 124*(6), 615-618.

Savenije, H. H. G. (2001), A simple analytical expression to describe tidal damping or amplification, *J. Hydrology, 243*, 205-215.

Savenije, H. H. G. (2005), *Salinity and Tides in Alluvial Estuaries*, Elsevier, 194 pp.

Savenije, H. H. G., and E. J. M. Veling (2005), Relation between tidal damping and wave celerity in estuaries, *J. Geophys. Res., 110*, C04007.

Schuttelaars, H. M., and H. E. de Swart (1999), Initial formation of channels and shoals in a short tidal embayment, *J. Fluid Mech., 127*, 15-42.

Seminara, G., and M. Tubino (2001), Sand bars in tidal channels. Part 1. Free bars, *J. Fluid Mech., 440*(1), 49-74.

Todeschini, I., M. Toffolon, G. Vignoli and M. Tubino (2003), Bottom equilibrium profiles in convergent estuaries, in *Proceedings of 3rd IAHR Symposium on River, Coastal and Estuarine Morphodynamics*, vol. 2, pp. 710-722, Barcelona (Spain).

Toffolon, M. (2002), Macro-scale morphological characterisation of the Western Scheldt, *Delft Cluster report 03.01.06*, Delft, the Netherlands (http://www.delftcluster.nl).

Winterwerp, J. C., Z. B. Wang, M. J. F. Stive, A. Arends, C. Jeuken, C. Kuijper, and P. M. C. Thoolen (2001), A new morphological schematization of the Western Scheldt estuary, The Netherlands, in *Proceedings of 2nd IAHR Symposium on River, Coastal and Estuarine Morphodynamics*, pp. 525-533, Obihiro (Japan).

Wolanski, E., K. Moore, S. Spagnol, N. DAdamo and C. Pattiaratchi (2001), Rapid, Human-Induced Siltation of the Macro-Tidal Ord River Estuary, Western Australia, *Estuarine, Coastal and Shelf Science, 53*, 717-732.

M. Toffolon and M. Tubino, Dipartimento di Ingegneria Civile e Ambientale, University of Trento, via Mesiano 77, 38050 Trento, Italy. (marco.toffolon@ing.unitn.it)

G. Vignoli, CISMA srl c/o BIC Südtirol, via Siemens 19, I-39100 Bolzano, Italy. (gianluca.vignoli@cisma.bz.it)

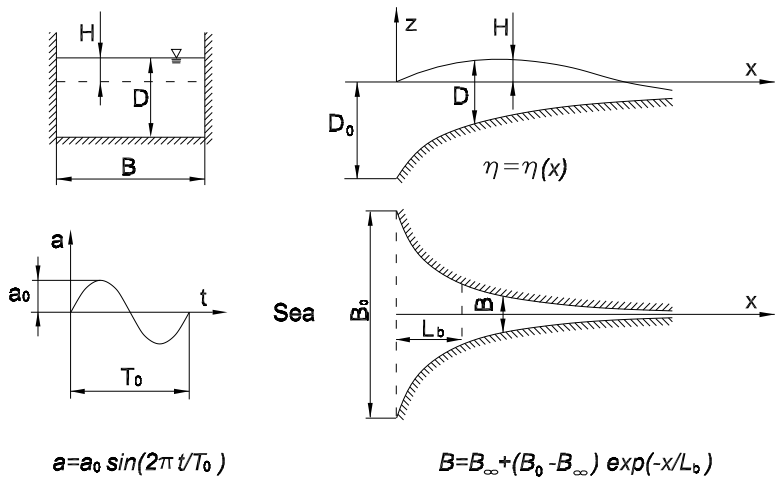

Figure 1. Sketch of the estuary and basic notation.

	Estuary	$a_0[m]$	$D_0[m]$	$L_b[km]$	C_h	$U_0[m/s]$	ε	χ	γ
1	Bristol Channel	2.6	45	6.3	14.0	1	0.06	0.48	2.30
2	Columbia	1	10	15.2	20.0	1	0.10	2.17	2.81
3	Conwy	2.4	3	20.6	20.0	0.5	0.80	52.9	6.17
4	Delaware	0.64	5.8	54	24.0	0.6	0.11	2.16	1.35
5	Elbe	2	10	56	19.2	1	0.20	3.52	1.68
6	Fraser	1.5	9	4.6	25.0	1	0.17	5.96	0.31
7	Gironde	2.3	10	87	14.4	1	0.23	5.00	1.60
8	Hudson	0.69	9.2	42	20.0	0.7	0.08	0.58	0.48
9	Ord	2.5	4	35	20.0 [a]	1.1	0.63	16.8	2.83
10	Outer Bay of Fundy	2.1	60	65	20.0	1	0.04	0.23	0.75
11	Potomac	0.65	6	230	21.0	0.9	0.11	1.71	1.01
12	Rotterdam Waterway	1	11.5	140	30.9	0.7	0.09	1.29	1.35
13	Western Scheldt	1.9	12 [b]	41 [b]	20.0 [b]	1 [b]	0.16	2.15	1.28
14	Severn	3	15	20	12.8	1.5	0.20	2.87	2.10
15	St. Lawrence	2.5	70 [c]	25	18.0	1	0.04	0.11	1.02
16	Tamar	2.6	2.9	25.5	20.0	0.5	0.90	18.9	8.30
17	Tees	1.5	7.5	217	19.2	0.4	0.20	6.14	10.7
18	Thames	2	8.5	42	19.2	0.6	0.24	8.96	2.57
19	Gambia *	0.6	8.7	40	21.8	-	0.07	1.42	1.17
20	Pungue *	3	4.3	34	20.0	-	0.70	45.9	2.31
21	Lalang *	1.5	10.6	60	21.8	-	0.14	2.63	0.33
22	Tha Chin *	1.35	5.3	50	19.2	-	0.25	11.9	0.59
23	Incomati *	0.5	3	5.5	16.0	-	0.17	5.83	0.92
24	Limpopo *	0.55	7	215	14.4	-	0.08	1.80	1.18
25	Maputo *	1.4	3.6	109	16.0	-	0.39	12.4	2.64
26	Chao Phya *	0.9	8	56	21.0	-	0.11	3.47	0.58

Table 1. The values of the tidal amplitude a_0, depth D_0, convergence length L_b, Chézy coefficient C_0 and characteristic measured velocity U_0 for some estuaries and the corresponding values of the dimensionless parameters ε, χ and γ. Data are taken from *Lanzoni and Seminara* [1998] and *Savenije* [2001] (denoted with *): [a] the value has been modified according to *Wolanski et al.* [2003]; [b] the values have been modified according to *Toffolon* [2002]; [c] the value ($7\,m$) of the reference depth reported in *Lanzoni and Seminara* [1998] seems unrealistic: our estimate is based on the original paper [*Prandle and Crookshank*, 1974].

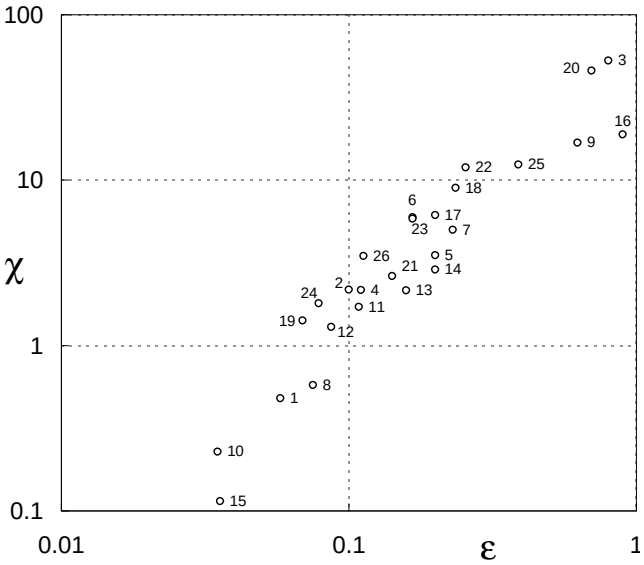

Figure 2. The relationship between the dimensionless parameters χ and ε for the estuaries listed in Table 1 is reported in a log-log plot.

Lanzoni and Seminara [1998]	ϵ	ψ	ϕ	K_0	R_0
Present paper	ε	$2\pi/\lambda$	μ	γ	χ/ε

Table 2. Correspondence of the most important symbols of the present paper with those used in *Lanzoni and Seminara* [1998].

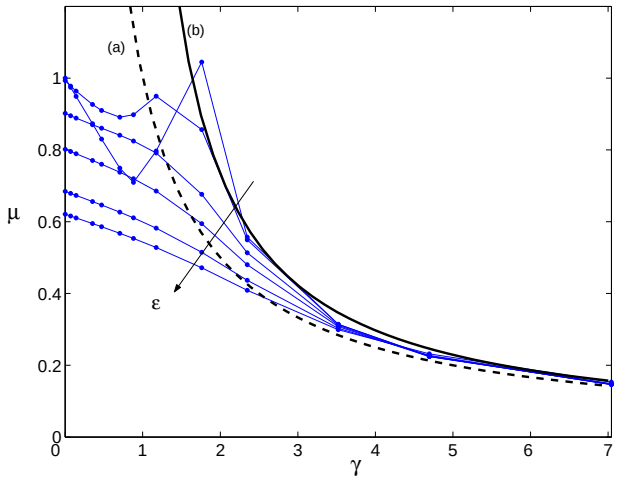

Figure 3. The dimensionless velocity scale μ is plotted as a function of γ for a strongly convergent and weakly dissipative channel. Numerical results (dotted lines) for different values of ε ($\varepsilon = 0.001, 0.01, 0.05, 0.1, 0.2, 0.3$), which correspond to the range $\chi = 0.016 \div 4.7$, are compared with theoretical estimates obtained through equation (22), (a) dashed line, and equation (23), (b) solid line ($a_0 = 0.01 \div 3\,m$, $D_0 = 10\,m$, $k_s = 45\,m^{1/3}s^{-1}$, $L_b = 10\,km \div \infty$, transparent boundary condition landward).

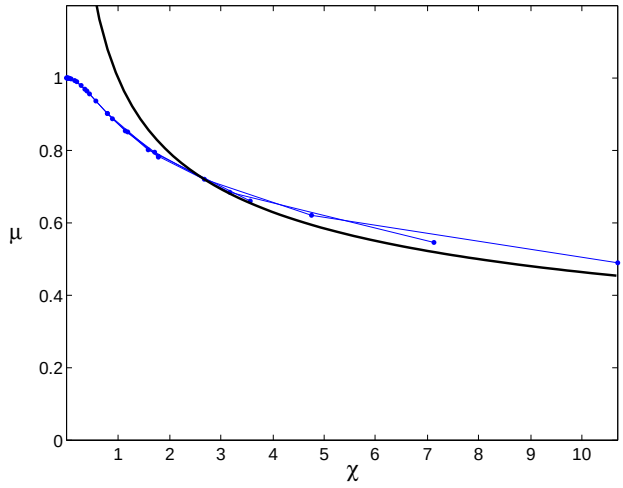

Figure 4. The dimensionless velocity scale μ is plotted as a function of χ for $\gamma = 0$ (constant width). The theoretical estimate obtained through equation (25) (solid line) is compared with numerical results (dotted lines) for different values of ε ($\varepsilon = 0.001, 0.01, 0.05, 0.1, 0.2, 0.3$): for a given ε, the values of χ correspond to different choices of k_s ($k_s = 30, 45, 60, 75, 90\, m^{1/3}/s$, $a_0 = 0.01 \div 3\, m$, $D_0 = 10\, m$, $L_b = \infty$, transparent boundary condition landward).

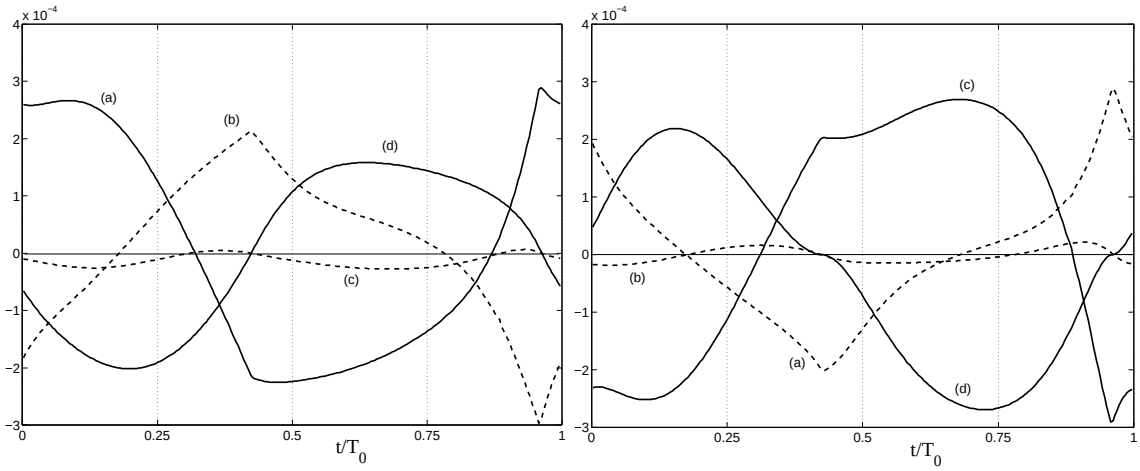

Figure 5. The relative importance of the various terms in the governing equations during a tidal cycle for a dissipative ($\chi = 3.2$) and convergent ($\gamma = 1.2$) channel: the test section is located $30\, km$ from the mouth of the estuary ($D_0 = 10\, m$, $a_0 = 2\, m$, $k_s = 45\, m^{1/3} s^{-1}$, transparent boundary condition landward).
(Left) Continuity equation (14): (a) $\frac{\partial H}{\partial t}$, (b) $D\frac{\partial U}{\partial x}$, (c) $U\frac{\partial D}{\partial x}$, (d) $-\frac{UD}{L_b}$ $[m/s]$. (Right) Momentum equation (13): (a) $\frac{\partial U}{\partial t}$, (b) $U\frac{\partial U}{\partial x}$, (c) $g\frac{\partial H}{\partial x}$, (d) gj $[m/s^2]$.

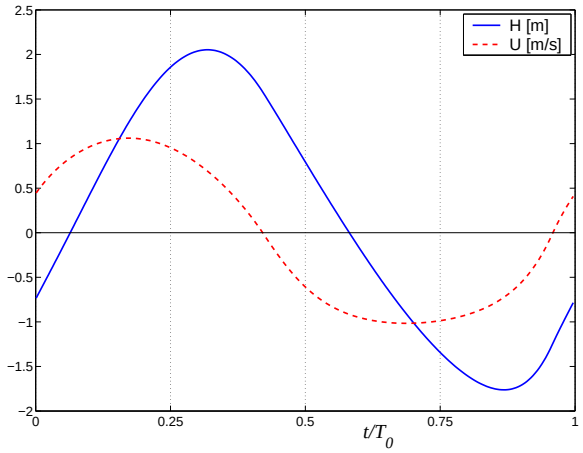

Figure 6. Wave characteristics during a tidal cycle: free surface level H (continuous line) and velocity U (dashed line) (data are the same as in Figure 5).

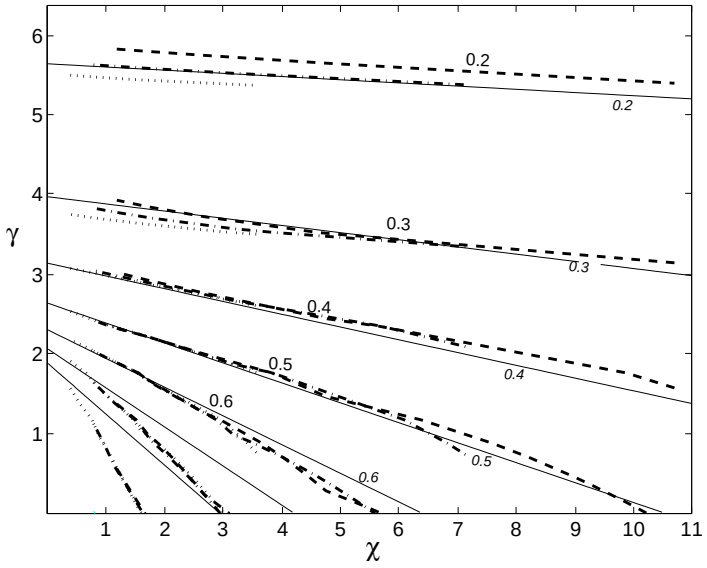

Figure 7. Contour plot of the dimensionless reference velocity μ in terms of the dimensionless parameters χ and γ: theoretical predictions from equation (28) (solid lines and numbers in italic) are compared with numerical results corresponding to different values of ε ($\varepsilon = 0.1$, dotted lines; $\varepsilon = 0.2$, dash-dot lines; $\varepsilon = 0.3$, dashed lines).

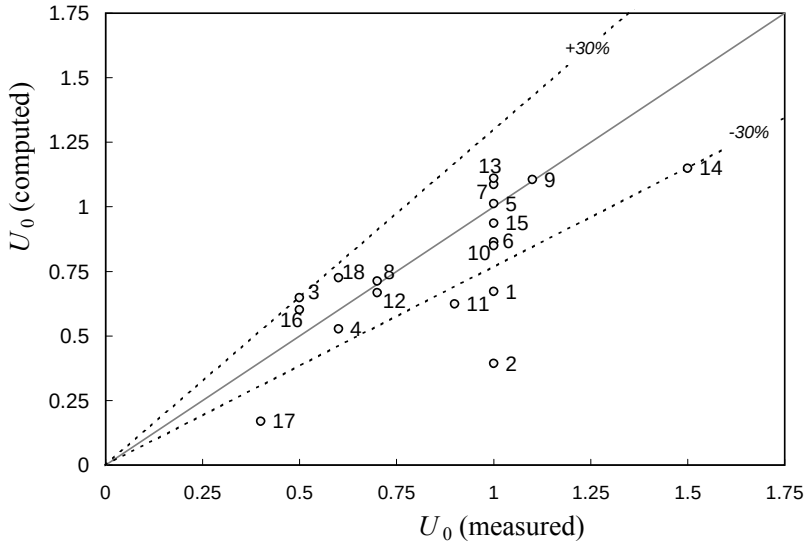

Figure 8. The scale of velocity computed through equation (28) is compared with measured values from Table 1 (numbers correspond to the estuaries considered).

S.&V.(2005) definitions	S.&V.(2005) notation	present paper notation	at the mouth ($x = 0$)
tidal amplitude	η	$\frac{H_{max}(x)-H_{min}(x)}{2}$	a_0
tidal velocity amplitude	υ	$\frac{U_{max}(x)-U_{min}(x)}{2}$	U_0
tidal average depth	$\overline{h}$	$\langle D(x) \rangle$	D_0
roughness coefficient	f	C_h^{-2}	C_0^{-2}
convergence length	b	L_b	
phase lag between HW and HWS	ϵ	α	
classical wave celerity	c_0	$L_g/T_0 = \sqrt{gD_0}$	
actual wave celerity	c	$L_0/T_0 = c_0/\lambda$	
damping scale of tidal range	$\delta_H = \frac{1}{\eta}\frac{d\eta}{dx}$		
damping scale of tidal velocity amplitude	$\delta_u = \frac{1}{\upsilon}\frac{d\upsilon}{dx}$		

Table 3. Notation used by *Savenije and Veling* [2005] and correspondence with the quantities defined in the present paper. Square brackets indicate average over the tidal period.

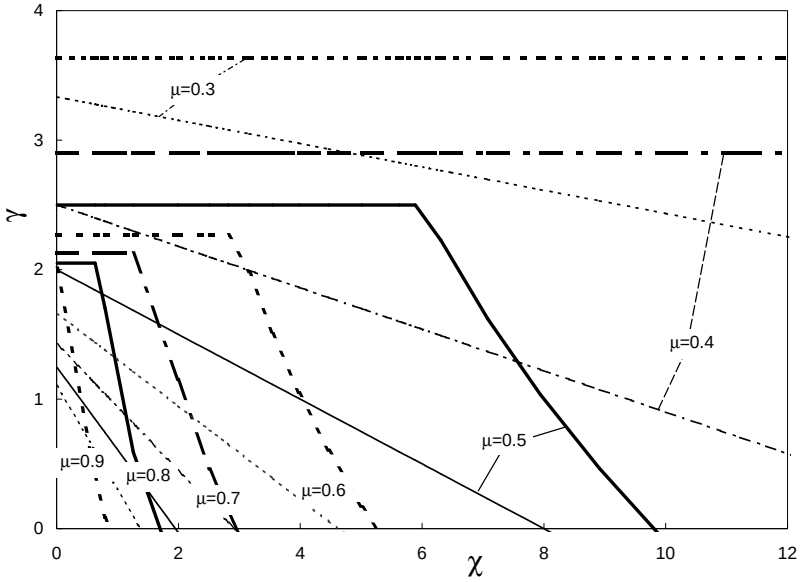

Figure 9. Contour plot of the dimensionless scale of velocity μ in the χ-γ plane. Bold lines: equations (37), (39); light lines: equation (28).

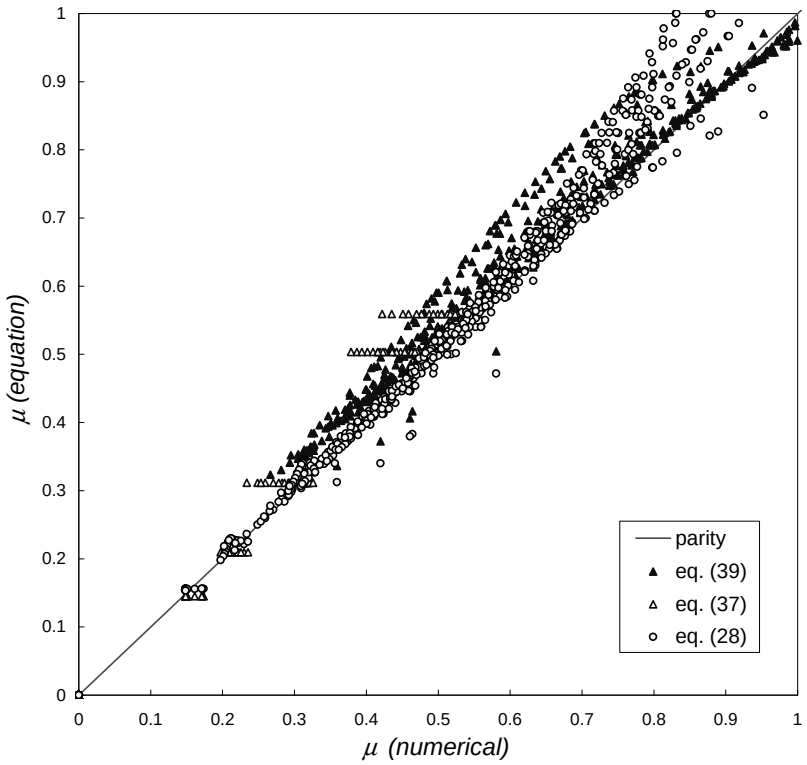

Figure 10. The analytical relationships for the dimensionless scale of velocity $\mu(equation)$ are tested against the numerical results $\mu(numerical)$. Triangles: equation (37); filled triangles: (39); circles: (28).

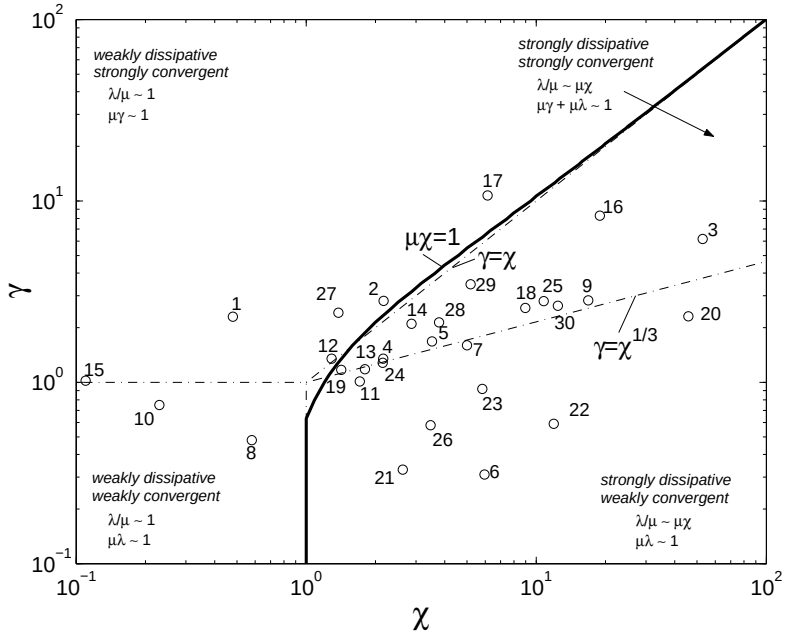

Figure 11. Estuarine classification in the plane (χ, γ) along with the regions of validity of asymptotic solutions: data from real estuaries from Table 1 are denoted by circles.

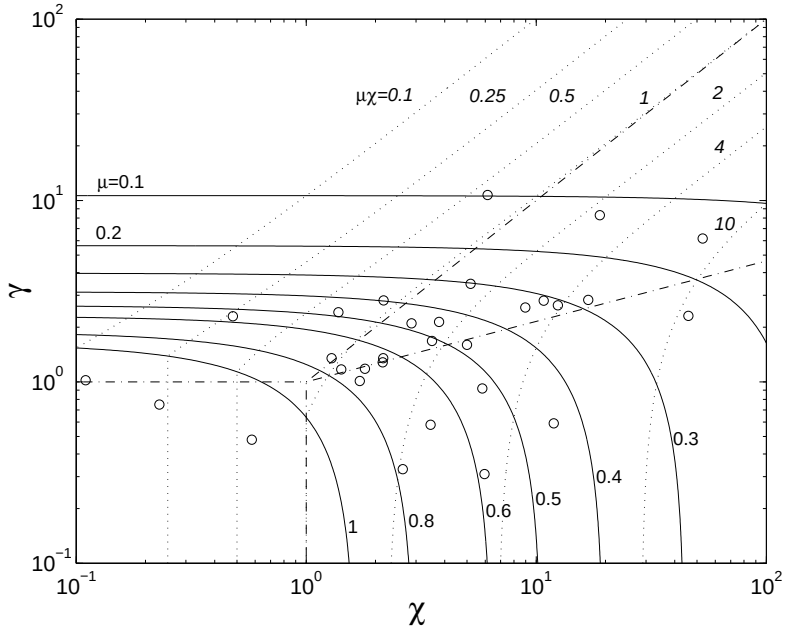

Figure 12. Contour plot of the dimensionless velocity μ (solid lines) and of the friction to inertia ratio $\mu\chi$ (dotted lines) obtained through (28): dash-dot lines and circles are the same as in Figure 11.

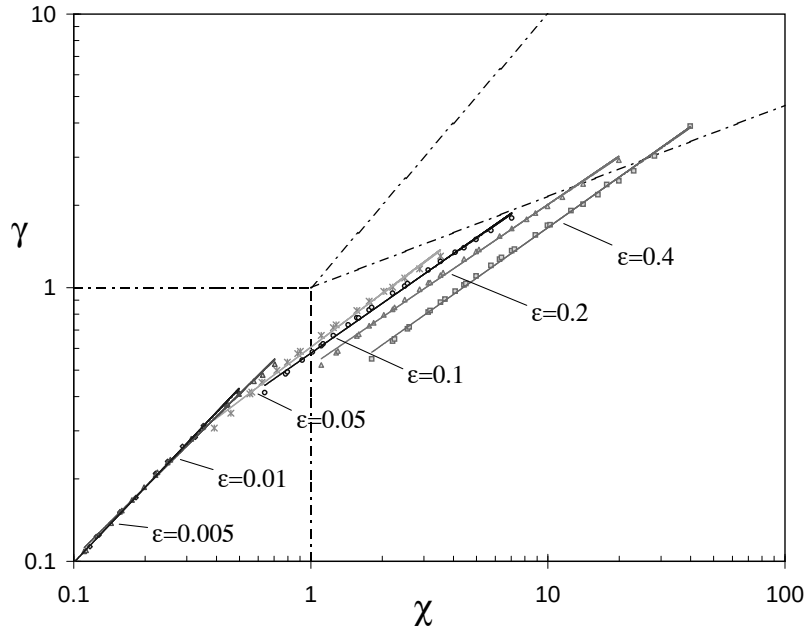

Figure 13. Marginal conditions for tide amplification in the χ-γ log-log plane, for different values of ε, as obtained with the numerical model. Points represent numerical runs, solid lines are the interpolating curve for given ε, dash-dot lines delimitate the regions introduced in Figure 11.

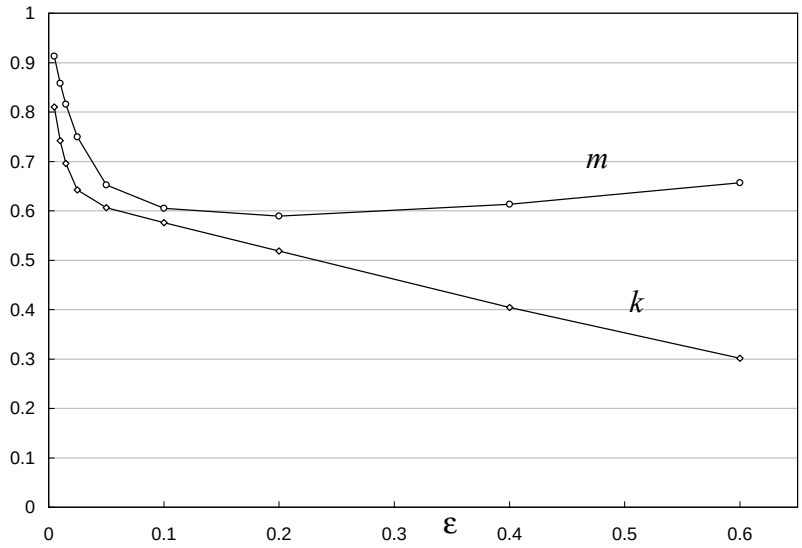

Figure 14. The coefficients m and k of equation (47) as functions of the dimensionless amplitude ε.

View publication stats

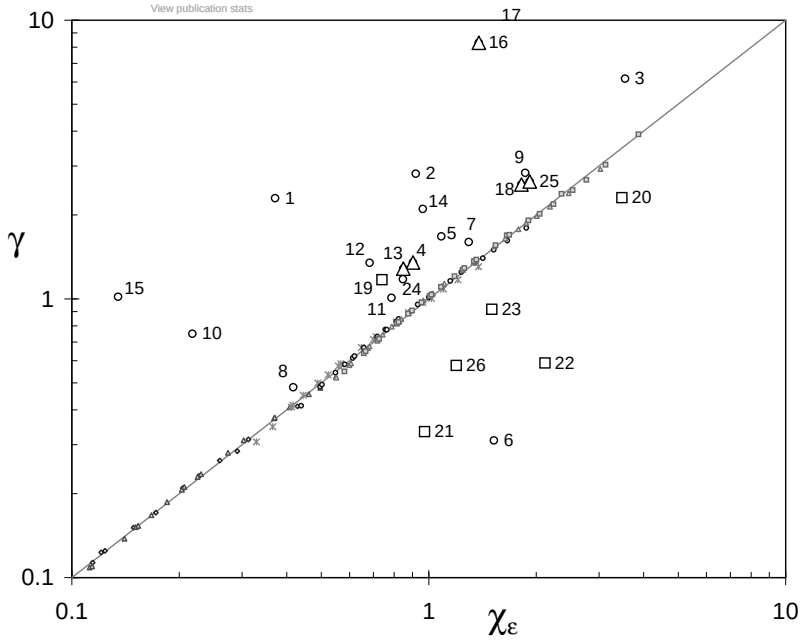

Figure 15. The marginal condition for tidal wave amplification is set in terms of the modified dimensionless parameter χ_ε defined in equation (48): data from real estuaries of Table 1 are represented using triangles where amplification is observed, squares for damping and circles when this information is not available.

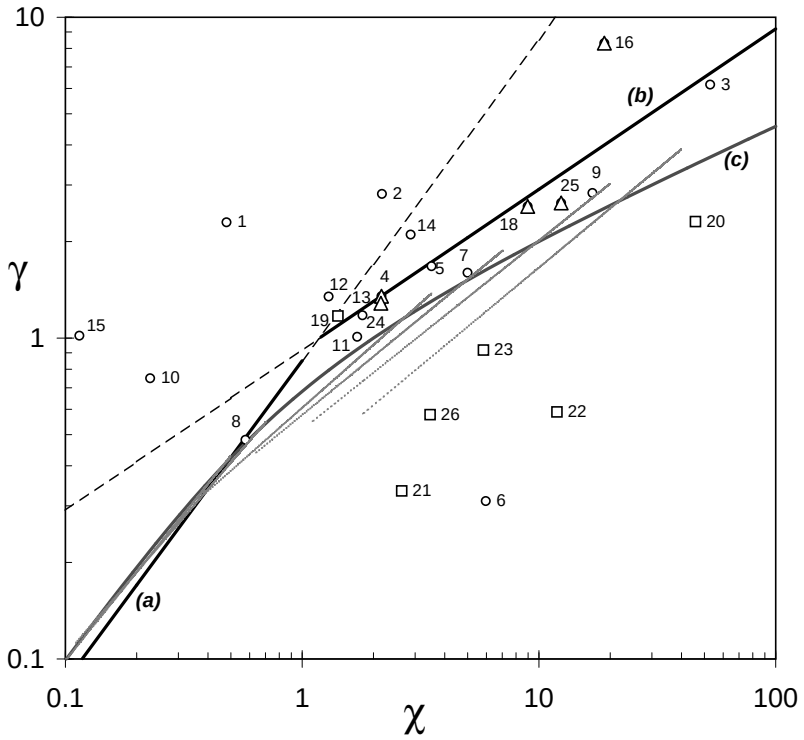

Figure 16. The marginal curves obtained through the analytical solutions of (*a*) *Lanzoni and Seminara* [1998], (*b*) *Friedrichs and Aubrey* [1994], and (*c*) *Savenije and Veling* [2005], are compared with those reported in Figure 13. Data from real estuaries of Table 1 are also included, using the same notation of Figure 15.